Capacity of interference exploitation schemes in multibeam satellite systems

Capacity of Interference Exploitation Schemes in Multibeam Satellite Systems

Alessandro Ugolini, *Member, IEEE*, Giulio Colavolpe, *Senior Member, IEEE*, Martina Angelone, Alessandro Vanelli-Coralli, *Senior Member, IEEE*, and Alberto Ginesi

***Abstract*—We propose a framework, based on the combined use of single- and multiuser detection, to jointly optimize the achievable rates of two signals sharing the same frequency in the forward link of a multibeam satellite system. We propose then the application of the described framework to two different scenarios of interest. First, we consider a uniform coverage scenario, aimed at maximizing the average throughput per beam in a realistic coverage condition. We compare different solutions, based on alternative frequency reuse schemes and different receiver strategies. We demonstrate that the use of multiuser detection can achieve significant gains over a reference strategy based on single-user detection. Next, we analyze a "hotspot" case, where resources are pulled from empty beams to serve a beam with a high service demand. Also in this case, we compare several strategies and frequency reuse schemes. We show that the best performance is achieved by a scheme adopting 3 colors and single-user detection.**

***Index Terms*—Multibeam satellite channels, multiuser detection, information rate analysis, multiple access channel.**

I. Introduction

Due to the explosion of the satellite services and applications experienced in the past few years, satellite operators have to face an increasing demand for high data rates and connectivity. In this context, satellite systems, widely adopted for broadcast transmission, can also be used for broadband unicast applications. A key example of this twofold use is represented by the second generation of the digital video broadcasting for satellite (DVB-S2) standard [1] and by its extension (DVB-S2X) [2], which are specifically designed to include also unicast services like, for example, internet access.

This request for high data rates has pushed the research community towards the study of more efficient ways to exploit the available bandwidth. The leading paradigm in the design of satellite communication systems has historically been based on *interference avoidance*. By transmitting signals that are separated in the time and frequency domains, it is ensured that a simple receiver structure can effectively recover the transmitted information. However, to provide a higher system capacity, and hence meet the increasing requirements, the attention of the research community has recently shifted towards the *interference management and exploitation* paradigm. Interference is not avoided by design any more, but a certain amount of controlled interference is intentionally introduced and mitigated or exploited, both at the transmitter and at the receiver sides, by the use of specifically designed transceiver architectures. Some examples of this change of paradigm can be found in [3]–[5] and references therein.

In satellite systems, the growing data rate request is satisfied by means of resource sharing, which is implemented by adopting a multibeam system architecture allowing to reuse the same bandwidth in different beams. In this scenario, interference arises from beams sharing the same frequency. Fig. 1 shows a typical 71-beam coverage of Europe, adopted by current broadcast and unicast systems. Different frequency reuse (FR) schemes can be used to cover the 71 beams, originating different levels of co-channel interference. One popular way to manage the interference in a multibeam satellite system is precoding [6], which has been shown in several studies to achieve excellent performance, from a theoretical point of view. However, there are also some practical aspects that need to be considered. The main problem of a practical implementation of precoding is that the transmitter needs the full knowledge of the channel state information, so its applicability is limited by the way estimates of the channels of the different interferers are obtained and fed back to the gateway. Clearly, precoding cannot be employed when the signals going to different beams come from different gateways.

Motivated by the aforementioned limitations, in this paper, we analyze the forward link of a multibeam satellite system for unicast applications, adopting different FR schemes, tackling the problem from a different point of view with respect to precoding. A 4-color scheme is the commonly adopted solution in most systems, as it ensures a low level of interference, whereas the more aggressive schemes, with a lower number of colors, ensure a more efficient usage of the bandwidth, at the price of an increased interference, which has to be managed to achieve the required performance. We consider the application of an advanced receiver, based on a multiuser detector (MUD) at the user terminals. Historically, the literature on MUD in the context of satellite communications has been concentrated on the study of the return link, from the user terminals to the terrestrial base station [7]–[13], where centralized techniques

This work is funded by the European Space Agency, ESA-ESTEC, Noordwijk, The Netherlands, under contract n. 4000116421/15/NL/FE ("Optimized Transmission Techniques for SATCOM Unicast Interactive Traffic"). The view expressed herein can in no way be taken to reflect the official opinion of the European Space Agency. This paper was presented in part at the Asilomar Conference on Signals, Systems, and Computers, Pacific Grove, CA, USA, Nov. 2016 and at the 14th International Symposium on Wireless Communication Systems, Bologna, Italy, Aug. 2017.

A. Ugolini and G. Colavolpe are with the Department of Engineering and Architecture, University of Parma, Italy (E-mail: alessandro.ugolini@unipr.it, giulio.colavolpe@unipr.it). M. Angelone and A. Ginesi are with the European Space Agency/European Space Research and Technology Centre, Noordwijk NL-2200 AG, The Netherlands (E-mail: martina.angelone@esa.int, alberto.ginesi@esa.int). A. Vanelli-Coralli is with the Department of Electrical, Electronic, and Information Engineering, University of Bologna, Italy (E-mail: alessandro.vanelli@unibo.it).

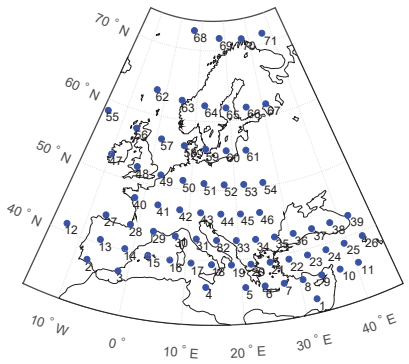

Figure 1. Typical 71-beam coverage of Europe. The numbered dots represent the centers of the beams.

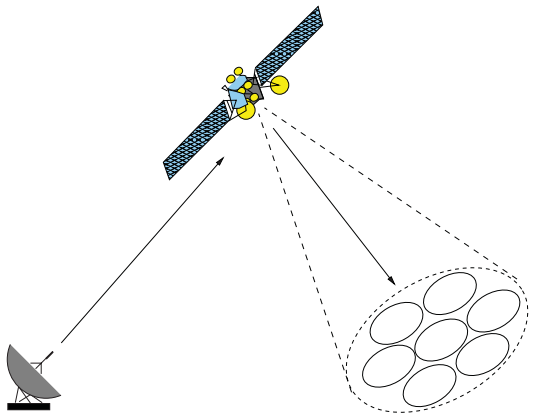

Figure 2. Forward link of a multibeam satellite system. Ellipses in the satellite service area represent beams, where user terminals are located.

are applied at the gateway.

The continuous technological evolution, however, allows to increase the complexity also at the user terminals, hence the application of a MUD becomes a feasible option also in the forward link, from the base station to user terminals. Note that, in this scenario, we assume user terminals to be fixed, and, hence, they can host a sufficient processing capability to equip receiver algorithms based on advanced signal processing techniques. Recent studies focused on a single beam [14]–[22] have shown that a MUD can significantly improve the detection performance when the user experiences a high level of interference, i.e., in an aggressive FR scheme. In particular, it was demonstrated in [14] that an advanced receiver, which adopts a MUD when it is convenient with respect to a classical single-user detector (SUD), can provide a very good performance in terms of achievable information rate (IR). In this paper, we extend the information theoretical framework of [14] to two users receiving two co-frequency signals, and we perform a joint evaluation of the achievable transmission rates. Unlike previous works in the literature, our analysis, hence, focuses on the whole system rather than on a single beam, resulting in a more complete performance evaluation. A system level analysis of the achievable rates has been proposed for wireless systems in [23], and first applied to satellite systems in [5], [24], [25]. Fig. 2 schematically shows the forward link of a multibeam satellite system. Signals are generated at the gateway (or at multiple gateways), then are sent to the multibeam satellite, which then forwards the signals to the beams on the surface of the Earth, where the user terminals are located, represented by ellipses in the figure.

We consider two different application scenarios to test the performance of the adopted information-theoretic framework. These scenarios have been demonstrated to be of interest for the satellite communications community, and they have not been analyzed before from a system level point of view. First of all, we focus on the maximization of the system capacity in a uniform coverage system, that is, where all the beams have the same FR scheme. In this scenario, the aim of our analysis is to maximize the average throughput per beam, and to compare the rates achievable by three alternative FR schemes (with 4, 2, and 1 colors, denoted as FR4, FR2, and FR1 schemes, respectively). The performance of the proposed framework is compared with that of a classical SUD system, and with a solution representing a more straightforward use of a MUD, which, as we demonstrate, is not the optimal solution. Unlike all previous researches, for this scenario we adopt a realistic channel model taking into account the typical impairments of a satellite communications scenario, i.e., real filters and nonlinear amplifiers, and realistic power profiles. This scenario is a generalization of that considered in [14], where the analysis is performed from the point of view of a single user, and under more simplified channel assumptions. The numerical results that we compute, as will be explained later, can be regarded as realistic performance bounds that are achievable using the proposed framework.

A different scenario, which has recently stimulated the interest of the satellite industry, where the proposed techniques are applied to improve the system flexibility, rather than to maximize the throughput, is what we call the "hotspot" scenario: we assume to have a beam with high service request surrounded by 6 beam with no request. We want to use the resources of the adjacent beams to serve the central beam, in order to meet its high throughput requirements. Also in this case, different FR and beam coverage schemes are compared. A similar problem has been recently studied also in [26]–[28], using different frameworks and techniques. In this paper, we apply our proposed framework to the same system model adopted in [26]–[28]. It is worth pointing out that, in this hotspot scenario, the different FR values might also represent different configurations of a flexible system with variable bandwidth per beam.

The paper is organized as follows. Section II introduces the main information theoretical framework, based on the use of a MUD and a SUD for two users sharing the same frequency. Section III analyzes the first scenario, where the proposed framework is applied to maximize the average throughput per beam. Section IV refers to the "hotspot" case, where resources from adjacent beams are used to increase the throughput of a single beam with high service demand. Finally, Section V concludes the paper.

II. Information Theoretical Framework

We assume to be in presence of two transmitters and two receivers, which share the same frequency bandwidth. Transmitter 1 sends message $x_1(t)$, intended for User 1, and Transmitter 2 sends message $x_2(t)$, intended for User 2. The two receivers observe signals $y_1(t)$ and $y_2(t)$, respectively. Depending on the adopted channel model, signals $y_i(t)$, $i = 1, 2$, can take into account all channel propagation effects, such as attenuation and nonlinear distortions in addition to the additive white Gaussian noise (AWGN). The information theoretical analysis is general and can be applied to any channel model. We assume that Transmitter 1 transmits with rate R_1 and Transmitter 2 transmits with rate R_2, and that all user terminals are equipped with an advanced receiver, which is able to perform both SUD and MUD operations.

It has been proved in [14], [15] that the achievable IR for a single user $i = 1, 2$ on a multiple access channel (MAC) is given by

$$R_i \leq \max\{I_{\mathrm{S}i}, I_{\mathrm{A}i}\}\,, \quad i = 1, 2\,, \tag{1}$$

where

$$I_{\mathrm{A}i} = \begin{cases} I(x_i; y_i|x_{3-i}) & \text{if } R_{3-i} < I(x_{3-i}; y_i) \\ I(x_i, x_{3-i}; y_i) - R_{3-i} & \\ & \text{if } I(x_{3-i}; y_i) \leq R_{3-i} < I(x_{3-i}; y_i|x_i) \\ 0 & \text{if } R_{3-i} \geq I(x_{3-i}; y_i|x_i) \end{cases}$$

is the maximum rate achievable when signal $3 - i$ can be perfectly decoded, and

$$I_{\mathrm{S}i} = I(x_i; y_i)$$

is the rate achievable by a SUD when signal $3-i$ is considered as additional noise. Using the same notation as in classical MACs, $I(x_i, x_{3-i}; y_i)$ is the rate achievable using a MUD at User i to jointly detect both received signals. $I(x_i; y_i|x_{3-i})$, instead, represents the rate achievable using a SUD at User i to receive signal i, assuming that the conditioning signal, $3-i$, has already been successfully received and canceled from the observable y_i. Finally, $I(x_i; y_i)$ is the rate achievable by a SUD at User i when the other incoming signal, indexed by $3 - i$, cannot be recovered.[1] From a practical point of view, the rate (1) means that the MUD receiver is adopted when it is convenient over the SUD. When the MUD receiver is adopted, the information intended for the other user is discarded after detection. When the SUD receiver is adopted, the other signal is considered as additional noise. This corresponds to an achievable rate region which differs from a classical MAC region because it is open on one side [14].

In this paper, we further extend this idea to evaluate the maximum rate jointly achievable by both receivers. The resulting achievable rate region is the intersection of the regions of the two users, each corresponding to an expression of the form (1). An example is reported in Fig. 3. The figure shows in red the IR achievable by User 1 and in blue that achievable by User 2. The joint region is given by the intersection of the two regions, which is shaded in the figure.

[1]The other combinations can be easily derived by exchanging the roles of the received signals and by considering User $3 - i$ instead of User i.

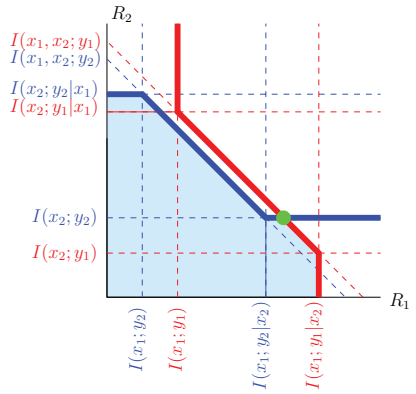

Figure 3. Joint achievable rate region for the MUD/SUD strategy.

We are interested in maximizing the overall sum-rate of the network (i.e., $R_1 + R_2$) and, if more pairs of rates achieve the maximum sum-rate, in minimizing the imbalance between the two rates (to ensure a certain level of fairness among the users). In the example shown, this corresponds to the green dot, whose rate is achieved with a MUD for User 1 and a SUD for User 2. In the rest of the paper, we will denote this solution as the "MUD/SUD" strategy. We point out that alternative metrics to the maximum sum-rate are possible. For example, maximizing the fairness in serving each user would be another interesting problem, which can be solved with the same tools, but selecting a different working point inside the joint achievable rate region.

The next sections study the application of the MUD/SUD strategy to some scenarios of interest in modern multibeam satellite applications, and compare its performance with other alternative techniques.

III. Scenario 1: Uniform Coverage

For the first scenario, we assume a uniform distribution of the request on the different beams. We consider a 71-beam coverage, as that shown in Fig. 1, and we focus our analysis on a generic pair of beams. This scenario has been preliminarly analyzed for the first time in [5], [29].

A. System Model

We consider two beams sharing the same frequency, and we serve one user from each beam, User 1 and User 2, respectively. Fig. 4 schematically reports the adopted channel model. Transmitter 1 transmits message $x_1(t)$ on the first beam, and Transmitter 2 transmits message $x_2(t)$ on the second beam. Depending on the adopted FR scheme, a significant level of co-channel interference can arise. The aim of this scenario is to compute the throughput of the two-beam system and to compare different transmitter and receiver strategies. Three different FR schemes will be applied in this section.

The terms γ_{ij}, $i = 1, 2$, $j = 1, 2$ in Fig. 4 are complex channel coefficients that take into account the position of each user inside the beam and the different antenna gains. The phases of γ_{ij} are uniformly distributed in $[0, 2\pi)$[2], and

[2]A joint optimization of the phases is, in principle, possible. However, the large number of considered beams makes the optimization problem unfeasible.

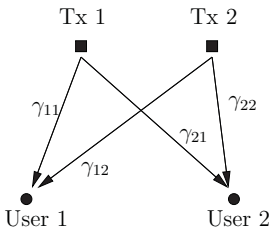

Figure 4. Considered channel model for the uniform coverage scenario.

the channel coefficients are assumed to be perfectly known at the receivers. This assumption is reasonable as long as a good phase estimator is available. This is not a problem if the estimate is made based on pilot symbols, present in all standards. The signals observed by the two users are

$$y_i(t) = \gamma_{i1} s_1(t) + \gamma_{i2} s_2(t) + w_i(t) + i_i(t) \quad i = 1, 2\,, \quad (2)$$

where $s_i(t)$ are the signals at the output of each transponder, possibly different from the transmitted signals, $x_i(t)$, due to the nonlinear transformation happening at the satellite transponder. Signals $w_i(t)$ are complex AWGN processes with power spectral density N_0, modeling the thermal noise of the channel, and terms $i_i(t)$ represent the further interference arising from beams outside the two-beam system, modeled as an additive Gaussian process with variance equal to the power of the interference.[3] The transmitted signals are obtained as the linear modulation of symbols belonging to classical phase shift keying/amplitude and phase shift keying (PSK/APSK) $M-$ary complex constellations, with $M = 4, 8, 16, 32$, possibly predistorted with the algorithm described in [30] and commonly used in DVB-S2 systems. They are modulated using a root raised-cosine pulse with roll-off factor 10%, and their symbol rate will be selected as a scaled version of the optimized values for a DVB-S2X system [2], according to the analysis reported in [31]. The considered satellite channel model is that foreseen by the DVB-S2 standard [1]. It is composed of an input multiplexer (IMUX) filter, a high power amplifier (HPA), and an output multiplexer (OMUX) filter, whose characteristics are provided in [1]. Single carrier per transponder operation and perfect timing alignment of the signals are assumed. Due to the single carrier per transponder assumption, we found it necessary to spend computational effort to perform our simulations on the described realistic channel model, rather than limiting our analysis to the linear channel and Gaussian symbols assumptions commonly adopted in the literature.

B. Adopted Receiver Strategies

We will compare different strategies that can be applied at user terminals. These techniques are based on the use of SUD and MUD receivers.

SUD receiver. The strategy based on a SUD receiver is the classical approach commonly adopted by user terminals. The receiver only tries to demodulate the information intended for the user, and all other signals are regarded as additional noise. One user is served in each time slot.

Time-sharing MAC. Both transmitters serve User 1 for a fraction α of the time interval, and User 2 for the remaining $1-\alpha$ fraction of the time interval. In this case, both received signals contain useful information for the user, which is split in two independent parts, each transmitted from a different antenna, hence both have to be detected with a MUD. This strategy represents a straightforward use of a MUD in a multibeam satellite system.

In the time slot for which the two signals are intended for User i, the channel becomes a classical MAC [32]. The two rates R_1 and R_2 have to be jointly selected to maximize the sum-rate. An example of rate regions for this case is shown in Fig. 5, where the two regions represent, respectively, the rates achievable in the two fractions of the time slot. In the reported example, it is assumed that the overall channel observed by User 1 (in red) is more favorable than that observed by User 2 (in blue). It is easy to show that, on a MAC, the maximum sum-rate achievable has the following expression

$$R_{\mathrm{MAC},i} = I(x_1, x_2; y_i)\,, \quad i = 1, 2\,.$$

The problem that now arises is how to select the fraction of time to be dedicated to each of the users. Different solutions can be applied. Clearly, the three discussed solutions are equivalent if and only if the two channels are identical.

- From the point of view of the overall sum-rate, the best solution is to serve for the whole time slot the user with the best channel (the red one in the example). This ensures that the maximum possible amount of information is transmitted. However, with this solution, the other user is not served at all. In this case, the overall sum-rate corresponds to

$$R_{\mathrm{MAC,best}} = \max(R_{\mathrm{MAC},1}, R_{\mathrm{MAC},2})\,. \quad (3)$$

- The simplest solution is to divide the time slot in two equal intervals, one for each user. This choice, however, results in a loss in the overall sum-rate if the two channels are not identical. The overall sum-rate, in this case, is

$$R_{\mathrm{MAC},50\%} = 0.5 R_{\mathrm{MAC},1} + 0.5 R_{\mathrm{MAC},2}\,.$$

- Another alternative solution is to allocate the time intervals so that the amount of transmitted information is the same for both users. This means that the fractions of time must be allocated so that they are inversely proportional to the achievable rate on each of the channels. In this case, the overall sum-rate is

$$R_{\mathrm{MAC,equal}} = \frac{2 R_{\mathrm{MAC},1} R_{\mathrm{MAC},2}}{R_{\mathrm{MAC},1} + R_{\mathrm{MAC},2}}\,.$$

MUD/SUD receiver. The MUD/SUD strategy described in Section II will be compared to the previously described alternative solutions. We can prove that the MUD/SUD strategy is always convenient with respect to the time-sharing MAC if some completely reasonable assumptions are satisfied. A proof to the following theorem can be found in Appendix A.

[3]Each term $i_i(t)$ approximates the sum of many contributions (the signals intended for the other beams), each with a power which is significantly lower than that of the useful signals. This sum of many small contributions can be considered as Gaussian with a good approximation level.

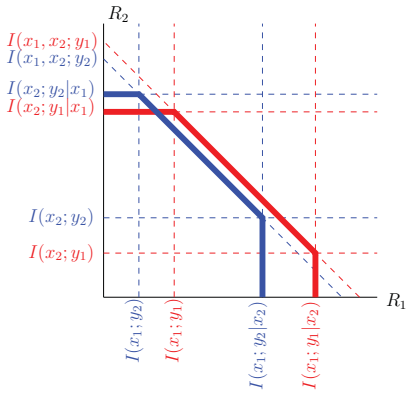

Figure 5. Achievable rate regions for the time-sharing MAC.

Theorem 1. *The MUD/SUD strategy, where the information for the co-channel beam is discarded after detection, achieves a sum-rate that is greater or equal with respect to the time-sharing MAC strategy, where both signals are used to serve the same user in a time division multiplexing way. This always happens when* $I(x_i;y_i) \geq I(x_i;y_{3-i})$, $i=1,2$, *that is, when the channel from Transmitter* i *to User* i *is better than the channel from Transmitter* i *to User* $3-i$.

Discussion. The condition $I(x_i;y_i) \geq I(x_i;y_{3-i})$, $i=1,2$ is totally reasonable in the scenario under consideration. In fact, in a uniform coverage scenario as that under consideration, a typical multibeam system is built in such a way that the signal transmitted from Transmitter i is intended to be received by User i in a specific beam. Hence, the same signal, when received by User $3-i$, which is located in a different beam, will experience worse propagation conditions, and its maximum achievable rate will be lower.

We point out that cooperation between the transmitters is needed in both the time-sharing MAC and the MUD/SUD strategies, because a joint selection of the transmission rates is performed in order to maximize the total sum-rate. However, in the considered scenario, the transmitters are located at the gateway, so this kind of cooperation is not a problem. On the other hand, no cooperation is needed between the ground users. To adopt the proposed strategies, the users simply have to feed back to the gateway the amplitude of the channel coefficients, which can be estimated by standard techniques, and changes very slowly due to the modification of the atmospheric conditions, and, hence, it is not critical. On the other hand, the possible use of precoding presents significantly more demanding channel estimation requirements, since also the phases of the channel coefficients have to be fed back to the transmitter in order to compute the precoding weights. These phases, in practical systems, change in a much faster way (due to the presence of the oscillators' phase noise) with respect to the amplitudes, hence the delay of this feedback can give rise to a significant performance loss.

C. Channel Characterization

We now describe the adopted FR schemes and define a common signal-to-noise ratio (SNR) reference. Let us define $B_{\text{ref}} = 500$ MHz the reference bandwidth for the computation of the throughput, $N = N_0 B_{\text{ref}}$ the noise power in the considered bandwidth, and let us also assume that the available power per beam is P_{b}. Notice that changing the value of B_{ref} would only impact the numerical values of the throughput, not the qualitative analysis, nor the relative performance ratio between the different techniques.

In this section, we define by $\text{SNR}^{(n)}$, $\text{Throughput}^{(n)}$, $T_{\text{s}}^{(n)}$, and $I_R^{(n)}$ the SNR, throughput, symbol time, and achievable IR per user for the FR scheme with n colors, respectively. Moreover, we define a power profile by sorting the users according to the power ratio between the useful signal and the most powerful interfering signal, C/I_1. For each value of C/I_1, we report the corresponding value of C, the power of the useful signal, and C/I_{res}, taking into account the residual interference coming from the other signals. Each C/I_1 value is paired with the corresponding probability of occurrence. The power profiles are computed as an average over the 71 beams of the coverage, generated by realistic system simulations performed at the European Space Agency in the framework of the project "Optimized Transmission Techniques for SATCOM Unicast Interactive Traffic", and are reported in Table I, where a quantization of C/I_1 in steps of 2 dB has been adopted[4]. The values of C provided in Table I shall be intended as the most probable signal power received by the users which experience a certain C/I_1 and they are therefore a variable contidioned to the interference level and not related to a specific geographical location. The actual probability density function (PDF) of the normalized C for each of the three scenarios is shown in Fig. 7, where we can notice that the FR2 and FR4 schemes have similar profiles (with a loss around 0.5 dB for the FR4 scenario due to the amplifier back-off) and that the FR1 distribution is about 3 dB lower due to the halving of the beam power over the two polarizations. Note that the values reported in Table I represent just an example of use case, and they can be affected by the change of different parameters, such as the number of beams and the adopted transmission bandwidth.

From the values in Table I, the amplitudes of the coefficients γ_{ij} and the variance of the residual interference $i_i(t)$ in (2) can be computed as

$$\begin{aligned} |\gamma_{ii}| &= \sqrt{10^{C/10}} \\ |\gamma_{ij,\, j\neq i}| &= \sqrt{10^{(C-C/I_1)/10}} \\ \text{var}\left\{i_i(t)\right\} &= 10^{(C-C/I_{\text{res}})/10}\,. \end{aligned}$$

The IR can be computed by means of the Monte Carlo technique described in [33]. If a suboptimal detector is applied, this technique allows to compute an achievable lower bound on the real IR, corresponding to the IR of the channel under consideration when that suboptimal detector is adopted, according to the principle of mismatched detection [34]. It is important to understand that treating the interference as noise allows to compute a lower bound to the (unknown) channel capacity which is **achievable** with the described strategy, which does

[4]The values of C in Table I have been normalized to their maximum value, in order to ensure a fair comparison among the three FR schemes. In this way, coefficients γ_{ii} can be regarded as attenuation factors, being always $|\gamma_{ii}| \leq 1$.

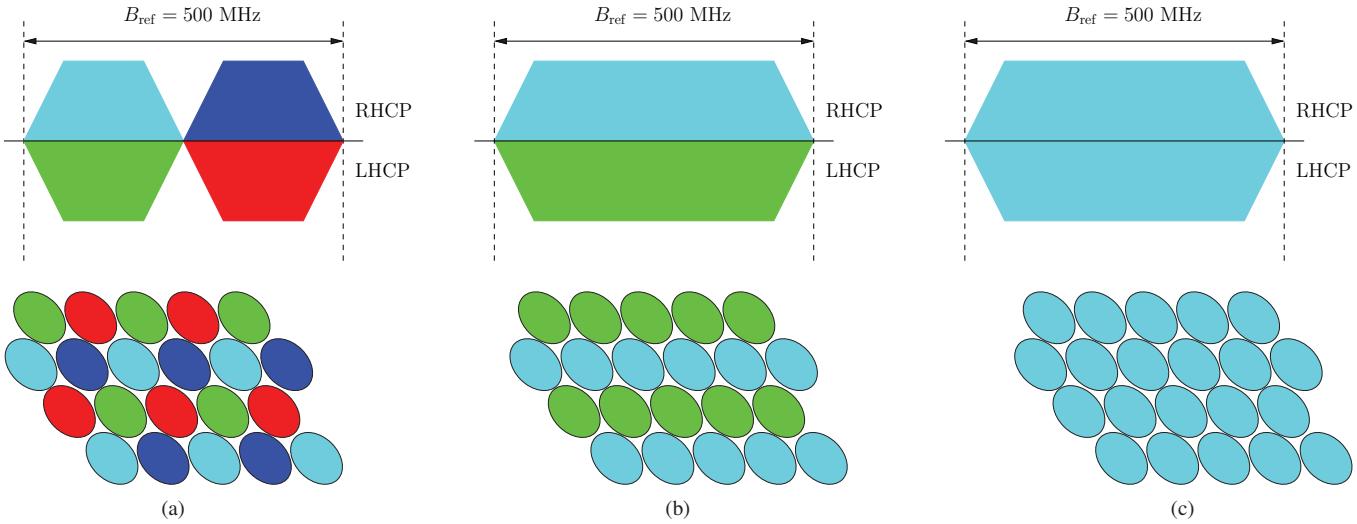

Figure 6. Bandwidth allocation and coverage for the FR4 (a), FR2 (b), and FR1 (c) scenarios.

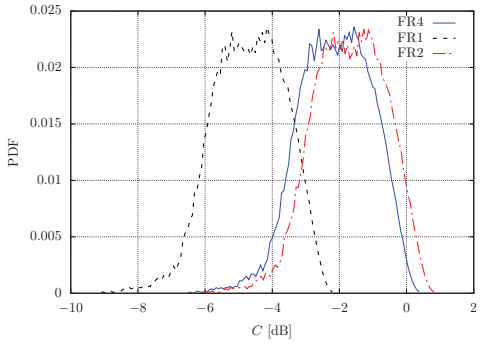

Figure 7. PDF of the normalized signal power C for the three FR schemes.

not attempt to jointly detect all interfering signals. Let us proceed with the description of the analyzed schemes, reported in Fig. 6, where RHCP and LHCP stand for right and left hand circular polarization, respectively.

The SNR and throughput can be expressed, for the three considered FR schemes, as

$$\text{Throughput}^{(n)} = \frac{2I_R^{(n)}}{nT_{\text{s}}^{(n)}} \quad [\text{bit/s}]\,, \tag{4}$$

$$\text{SNR}^{(n)} = \frac{nP_{\text{b}}}{2N}\,. \tag{5}$$

Four colors scheme (FR4). Fig. 6(a) represents the bandwidth allocation and the beam coverage for a typical four colors scheme, the classical solution in current satellite systems. Signals occupy half of the available bandwidth and the factors 2 in (4),(5) depend on the fact that the bandwidth assigned to each user is half of the total available bandwidth, halving both IR and noise power. The selected symbol rate for each signal is 243.5 Mbaud with OMUX filters with bandwidth 250 MHz [31]. To generate the power profile, the beam is divided into 8 regions, labeled $P_0, \ldots, P_7$.

Two colors scheme (FR2). A FR2 scheme is reported in Fig. 6(b). The two signals occupy the whole available bandwidth and, for an OMUX bandwidth of 500 MHz, the selected symbol rate is 487 Mbaud [31]. The beam, in this case, is divided in 7 regions according to the C/I_1 values.

One color scheme (FR1). Fig. 6(c) shows the bandwidth allocation and coverage for a full-frequency reuse scheme. Notice that the same user is served by both polarizations. In this case, the factors 2 in (4),(5) take into account that both polarizations are used to serve the same user, doubling the IR and halving the power per polarization. Again, the adopted symbol rate is 487 Mbaud, and the power profile is divided into 7 regions. We notice that this scenario experiences a much higher level of interference than the others.

For the FR4 scheme, we have a total of 64 possible combinations of the positions of two users in the two beams (some of which are symmetric if we exchange the roles of the beams). For the FR2 and FR1 schemes, instead, we have 49 possible combinations. We will evaluate the throughput for each combination with the three strategies described previously, and then average the results to obtain the average throughput per user with the three schemes. By observing the power profiles in Table I, we see that the interference observed in the FR4 case is very low, making the use of a MUD receiver not convenient. A MUD for the two most powerful signals, instead, can be beneficial for FR2 and FR1. We see that, for FR1, also the residual interference has a significant contribution; in this scenario, a MUD for 3 or more signals would ensure better performance but, due to the exponentially increasing number of cases, this solution has not been considered.

D. Numerical Results

In this section, we discuss the performance of the presented techniques with the three FR schemes. The FR4 case with a SUD receiver will be used as a reference to compare the other techniques, being the solution adopted by classical user terminals. All numerical results have been obtained by providing a sufficient averaging over the phase values. The

Table I
POWER PROFILES FOR THE THREE FR CASES.

		P_0	P_1	P_2	P_3	P_4	P_5	P_6	P_7
C [dB]	FR4	-1.4	-2.5	-2.5	-2.8	-3.1	-2.6	-2.5	-3
	FR2	0	-0.5	-0.5	-1	-1.5	-2	-2.5	-
	FR1	-2.5	-3	-3	-3.5	-4	-5	-5.5	-
C/I_1 [dB]	FR4	26	24	22	20	18	16	14	12
	FR2	12	10	8	6	4	2	0	-
	FR1	12	10	8	6	4	2	0	-
C/I_{res} [dB]	FR4	24	23	22	22	21	20	20	29.5
	FR2	13.1	12.9	13.5	14.5	14.8	13.8	12.9	-
	FR1	6.1	5.8	4.9	4.3	2.9	1.3	-0.3	-
Probability	FR4	0.6733	0.1393	0.0918	0.0555	0.0259	0.0095	0.0041	0.0005
	FR2	0.1289	0.1817	0.1773	0.1653	0.1526	0.1349	0.0593	-
	FR1	0.0207	0.0591	0.1095	0.1625	0.2152	0.2736	0.1593	-

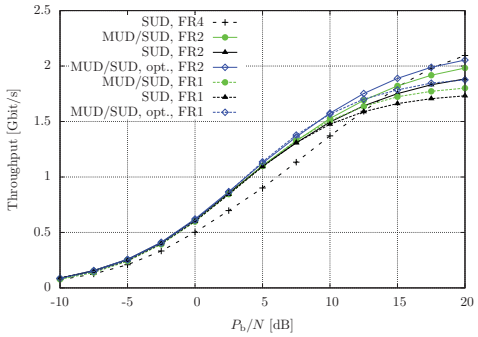

Figure 8. Throughput achievable for the MUD/SUD strategy.

presence of interfering signals other than I_1 has been taken into account by adding an additional noise process with power given by the overall power of the interfering signals, according to the model (2). We compute the average throughput per user, by selecting the constellation and the back-off of the HPA which ensure the highest value for each SNR.

At the receiver, a sufficient statistic for detection is extracted by means of oversampling at the output of a front-end filter [35]. A fractionally-spaced minimum mean square error (FS-MMSE) equalizer is used as an adaptive filter, followed by a symbol-by-symbol detector (single- or multiuser). This receiver structure does not rely on any specific signal model and, hence, it is fully adaptive. When the MUD is adopted, the equalizer jointly operates on all the signals to be detected.

Fig. 8 reports the throughput for the MUD/SUD strategy, that is, using a MUD when it is convenient over a SUD, for the FR2 and FR1 schemes. The performance of this strategy is compared with the throughput achievable when using only a SUD in the same FR schemes, and with the reference curve of the SUD for the FR4 scheme. We see that there is a large SNR range in which the FR2 and FR1 solutions have similar performance and they exhibit a significant gain around 2 dB over the classical FR4 scheme. If we compare FR2 and FR1, we see that the SUD receiver has similar performance in the two cases, with the FR1 saturating earlier due to the higher level of interference. The same behavior is observed also when the MUD/SUD receiver is adopted. For both schemes, the MUD starts gaining over the SUD from a SNR of 5 dB, with a power gain of about 0.6 dB for FR1 and 0.4 dB for FR2, at 1.5 Gbit/s. It is also worth mentioning that 32APSK is never selected by the FR2 and FR1 schemes, and this explains why the FR4 curve crosses the others at high SNR. We point out that these results might slightly change if higher order constellations, like 64APSK, 128APSK and 256APSK, were adopted. Due to the high complexity of the MUD approach, we have not simulated these cases. However, we could reasonably expect an improvement of the maximum throughput achievable by all techniques, without significant changes in the relative performance of the different strategies.

As mentioned, these results have been obtained by averaging the throughput over all combinations of the users' positions. An improvement can be achieved by pairing the users in a smarter way. We made the assumption of 100 users in each beam, with a C/I_1 distribution as in Table I. We used the Hungarian algorithm [36], which is the optimal algorithm to solve this assignment problem, i.e., which of the users in the second beam should be paired with each user of the first beam to maximize the throughput. The resulting assignment is shown in Fig. 9 for $P_{\text{b}}/N = 10$ dB and the FR2 scheme. In the figure, the dashed lines divide the users according to their C/I_1 value, and the coordinates of the points denote the two users that should transmit at the same time. Note that there is exactly one point for each row and for each column, and that there is a clear symmetry in the assignment. This optimization allows to select the cases in which the MUD/SUD receiver provides the highest advantages. The results are reported in Fig. 8, labeled as *MUD/SUD, opt.*, and they show a gain of about 0.6 dB for FR2 and 0.8 dB for FR1 over the average on all positions, at 1.5 Gbit/s.

Fig. 10 reports the throughput achievable with the time-sharing MAC strategy. We can clearly see that the MUD/SUD receiver leads to better performance, as also foreseen by the theoretical analysis. Then, we notice that FR1 has a slightly better performance than FR2 at medium SNR, but the curves saturate earlier. We have verified that optimizing the assignment of the users ensures some extra limited gains, but time-sharing MAC cannot outperform the reference curve of the FR4 scheme.

IV. SCENARIO 2: HOTSPOT

A different scenario, in which advanced techniques can be used not to increase the system capacity or throughput, but to improve the system flexibility, is described in this section. We

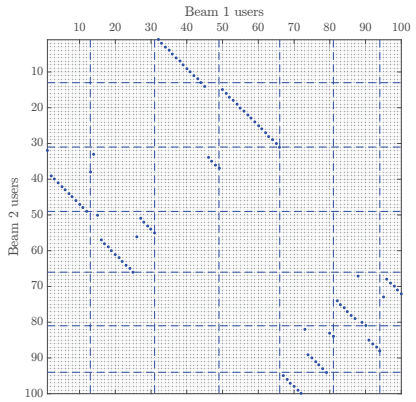

Figure 9. Optimal assignment of 100 users in the two beams for the MUD/SUD strategy and FR2 for $P_{\rm b}/N = 10$ dB.

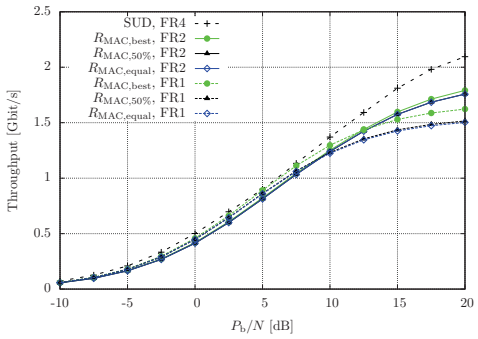

Figure 10. Throughput achievable for the time-sharing MAC.

consider a cluster of 7 beams and we assume that the central beam of the cluster is "hot", that is, it has a high service requirement, while the 6 surrounding beams are "cold", that is, they have no service requirement at all. This is clearly an abstraction, but it is useful to draw some conclusions on the applicability of different techniques, involving the comparison of different FR schemes and receiver architectures. We refer to this scenario as to the "hotspot" scenario. The problem of the hotspot has been tackled recently in [26], where the authors compare alternative capacity measures for a multibeam scenario, in [27], which takes into account the application of code-division multiplexing, and in [28], which tackles the problem from the point of view of precoding. The idea behind this analysis is to draw resources, namely bandwidth and power, from the 6 cold beams to serve users in the central beam. It does not make sense to extend the hotspot to more beams. In fact, the outer beams (those outside the ring of 6 beams already considered) have a very limited impact on the central beam.

For this study, we concentrate on a cluster centered on beam 42 of the European coverage, as shown in Fig. 11, so that the 6 adjacent beams are numbers 30, 31, 41, 43, 49, and 50. Our aim, in this case, is to understand the specific behavior inside a single beam of interest, rather than an average behavior on the whole coverage. For this reason, the quantization of the power levels inside the beam is much finer than in the uniform coverage scenario. For this reason, we have a much larger number of cases to analyze, and the

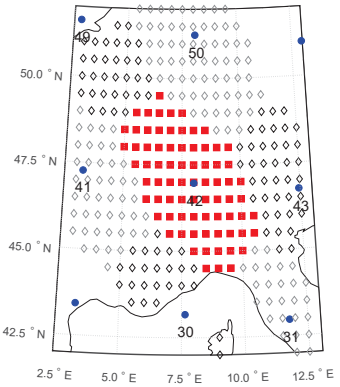

Figure 11. Cluster of 7 beams considered for the hotspot analysis.

computational complexity required to run simulations in this scenario does not allow us to obtain results with discrete constellations and a more realistic channel model. Hence, the adopted channel model is a linear AWGN channel. For the same reasons, the analysis is carried out under the assumption of Gaussian symbols and interference (the same assumptions adopted in [26]–[28], which is totally reasonable in a multiple carriers per transponder scenario, as that under consideration in this case). All beams outside the hotspot of 7 beams have a bandwidth allocation corresponding to a 4 colors scheme. We assume that all users are served using both polarizations, and that the total available bandwidth is $B = 500$ MHz. There are $N_{\rm u} = 76$ users in the considered beam, represented by the squares in Fig. 11, and for each user there are $N_{\rm int}$ interfering signals coming from other beams. For each user i, we denote by $C^{(i)}$ the power of the signal coming from the central beam, by $N^{(i)}$ the observed noise power, and by $I_j^{(i)}$, $j = 1, \ldots, N_{\rm int}$ the power of each of the interfering signals. We assume that $I_j^{(i)} \geq I_{j+1}^{(i)}$ $\forall j$. Also for this scenario, the power profiles for all users have been generated at the European Space Agency in the framework of the project "Optimized Transmission Techniques for SATCOM Unicast Interactive Traffic". The full set of data is available online at [37]. The next subsections describe the adopted solutions.

The cases with 7 and 6 users served together, which will be analyzed next, arise naturally from the geometry of the problem. Clearly, there are not only 7 or 6 users in the hotspot, but just 7 or 6 served at the same time, in a time-division fashion.

A. Reference Scenario

The reference scenario assumes a uniform 4-color distribution on all the coverage. There is no hotspot in this case, and each beam is assigned the same amount of resources. The level of interference observed by the signals is very low thanks to the adopted FR scheme. All users adopt single-user detection, and the achievable rate for each user i can be expressed as

$$I_R^{(i)} = \log_2 \left(1 + \frac{C^{(i)}}{N^{(i)} + \sum_{j=1}^{N_{\rm int}} I_j^{(i)}} \right) . \qquad (6)$$

The throughput for each user is then computed as

$$\text{Throughput}^{(i)} = I_R^{(i)} 2B/4 \quad [\text{bit/s}] ,$$

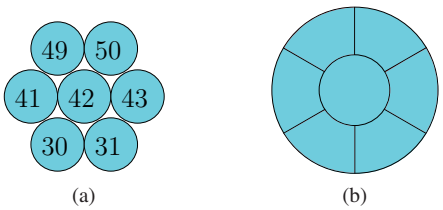

(a) (b)

Figure 12. Frequency reuse scheme (a) and beam coverage (b), for the MUD/SUD with 7 users.

where the factor 2 takes into account that both polarizations are used to serve the user, and the division by 4 is due to the fact that, in a 4-color scheme working on two polarizations, each user is assigned $1/4$ of the available bandwidth. The average throughput is computed by averaging the values of $\text{Throughput}^{(i)}$ of all users, and it results in

$$\text{Throughput}^{(\text{Reference})} = 1.32 \text{ Gbit/s}\,.$$

B. Hotspot SUD

In this scenario, the central beam is assigned also the bandwidth of the adjacent beams, so that the bandwidth available for the central beam is 4 times larger than in the reference case. The 6 adjacent beams are switched off and, for this reason, the level of interference experienced by the signals is very low. Hence, also in this case, the users will perform single-user detection, and we can compute the rate achievable by each of the users as in (6), and the throughput for each user as

$$\text{Throughput}^{(i)} = I_R^{(i)} 2B \quad [\text{bit/s}]\,, \tag{7}$$

where the factor 2 again takes into account that both polarizations are exploited to serve the user. Finally, the average throughput in the beam is computed by averaging the values of $\text{Throughput}^{(i)}$ of all users. The average value of the throughput over all users is

$$\text{Throughput}^{(\text{Hotspot SUD})} = 5.23 \text{ Gbit/s}\,.$$

C. MUD/SUD with 7 users

As in the previous scenario, also here we assign more bandwidth to the central beam, so that its available bandwidth is 4 times larger with respect to the reference scenario. However, instead of switching off the adjacent beams, we use them to serve part of the users. In particular, we assume that the users in the inner part of the beam are served by the signal coming from the central beam, while the users in the outer sections of the beam are served by the signals coming from the adjacent beams (which transmit on the same bandwidth, with a full frequency reuse scheme). The size of these areas is determined by looking at the values of C/I_1. The users observing a C/I_1 larger than a fixed threshold belong to the central section, the others to the outer sections. A schematic representation of the beam coverage is reported in Fig. 12. The values of C/I_1 are much lower than those of the previous scenario [37].

To cope with the increased interference, all users can adopt the MUD/SUD strategy for the two most powerful signals. After detection, the data stream intended for the other user is discarded, as it does not carry useful information.

Let us consider the user in the central area and the outer user whose signal has the highest level of interference for the central user. Let us denote by x_1, the signal transmitted by the central beam with rate R_1, and by y_1 the signal received by the central user (user 1). Similarly, let us denote by x_2 the signal transmitted by the adjacent beam with rate R_2, and by y_2 the signal received by the outer user (user 2). For the central user, we can compute the following rates:

$$I(x_1, x_2; y_1) = \log_2 \left(1 + \frac{C^{(1)} + I_1^{(1)}}{N^{(1)} + \sum_{j=2}^{N_{\text{int}}} I_j^{(1)}} \right), \tag{8}$$

$$I(x_1; y_1 | x_2) = \log_2 \left(1 + \frac{C^{(1)}}{N^{(1)} + \sum_{j=2}^{N_{\text{int}}} I_j^{(1)}} \right), \tag{9}$$

$$I(x_1; y_1) = \log_2 \left(1 + \frac{C^{(1)}}{N^{(1)} + \sum_{j=1}^{N_{\text{int}}} I_j^{(1)}} \right). \tag{10}$$

The rate (8) represents the rate achievable by a MUD for the useful signal and the most powerful interfering signal. The rate (9) is the rate achievable by a SUD in the assumption of perfect detection of the interfering signal (which can then be canceled), and (10) is the rate achievable by a SUD when all interfering signals are considered as additional noise. With similar steps, we can compute the following rates for the outer user:

$$I(x_2, x_1; y_2) = \log_2 \left(1 + \frac{I_1^{(2)} + C^{(2)}}{N^{(2)} + \sum_{j=2}^{N_{\text{int}}} I_j^{(2)}} \right), \tag{11}$$

$$I(x_2; y_2 | x_1) = \log_2 \left(1 + \frac{I_1^{(2)}}{N^{(2)} + \sum_{j=2}^{N_{\text{int}}} I_j^{(2)}} \right), \tag{12}$$

$$I(x_2; y_2) = \log_2 \left(1 + \frac{I_1^{(2)}}{N^{(2)} + C^{(2)} + \sum_{j=2}^{N_{\text{int}}} I_j^{(2)}} \right). \tag{13}$$

Rates (8)–(13) define the joint achievable rate region for the MUD/SUD strategy (see Section II and Fig. 3). If there are more points of the region which maximize the sum-rate, as is the case in the example in Fig. 3, we select the combination which maximizes R_2 and minimizes R_1. The reason behind this choice will become clear when we consider also the signals coming from the other 5 outer beams. Again, this corresponds to the green point in the figure.

Let us now extend the analysis to signals x_k, $k = 3, \ldots, 7$, coming from the other 5 adjacent beams. Similarly to what we did for user 2, we can define rates equivalent to (11)–(13) by replacing index 2 with k.

Rates (11)–(13) define, for each user, an achievable rate region similar to the blue region in Fig. 3. However, in this case, we cannot jointly select the rates because R_1 has already been fixed (and selected jointly with R_2). Hence, the rates R_k, $k = 3, \ldots, 7$ are selected by taking the point of the border of their region with abscissa R_1. We can now motivate the selection of the pair of rates which minimizes R_1: this choice maximizes all rates R_k, $k = 2, \ldots, 7$, and ensures the highest

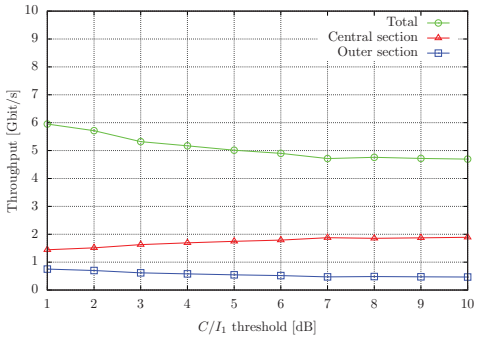

Figure 13. Throughput as a function of the C/I_1 threshold for the inner and outer sections in for MUD/SUD with 7 users.

possible sum-rate. The total achievable rate for a configuration ℓ of 7 users is then simply computed as

$$I_R^{(\ell)} = \sum_{k=1}^{7} R_k \,, \tag{14}$$

and the throughput for this configuration of users is expressed as in (7). After a sufficient average on the users' positions, we can evaluate the average throughput for each value of the adopted C/I_1 threshold, which, we remind, define the size of the central area of the beam. The throughput as a function of the C/I_1 threshold is reported in Fig. 13, which also shows the average throughput of the central and of one of the outer sections. We see that the choice that maximizes the total throughput also minimizes the difference between the sections. We define as the throughput of this strategy the maximum over the C/I_1 threshold of the computed values,

$$\text{Throughput}^{(\text{MUD/SUD 7 users})} = 5.95 \text{ Gbit/s}\,.$$

We see that the throughput increases as the threshold decreases, meaning that it is convenient to serve a large region of the beam with the central signal. Notice that, however, it is not convenient to serve the whole beam with the central signal, as we would lose the capacity arising from the use of the adjacent beams. To fully exploit the available resources, there must be a share of the users, although small, which is served by the external beams.

D. Three-color SUD

This scenario assumes a 3-color scheme on the hotspot beams. The central beam is again divided in 7 areas, each served by one of the beams, as reported in Fig. 14. However, unlike the previous scenarios, the interference pattern is different. In fact, due to the 3-color scheme, the values of interference are very low, which makes the use of a MUD not convenient. All users, hence, will adopt a single-user receiver. This strategy is applied also in [26], although with different assumptions concerning the power profiles. For all users, we will assume that the power ratio between the signal coming from the central beam and the sum of all interfering signals from outside the hotspot is fixed to $C/I_{\text{res}} = 26$ dB. This value is computed as an average of the interference coming from the beams which do not belong to the hotspot.

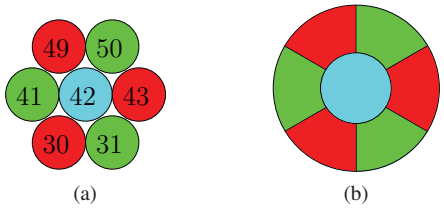

(a) (b)

Figure 14. Frequency reuse scheme (a) and beam coverage (b), for the 3-color SUD.

Let us concentrate on a configuration ℓ of 7 users, one from each section. Let us denote again by R_1 the rate of the signal transmitted on the central beam, and by R_k, $k = 2, \ldots, 7$, the rates of the signals transmitted by the 6 adjacent beams. The rate achievable by the user in the central section is

$$R_1 = \log_2 \left(1 + \frac{C^{(1)}}{N^{(1)} + I_{\text{res}}^{(1)}} \right) .$$

We notice that for the central users, there are no interfering beams inside the hotspot, and the only interference is the residual term from outside the hotspot. For the other 6 users, we can define the achievable rates as

$$R_k = \log_2 \left(1 + \frac{I^{(k)}}{N^{(k)} + I_{\text{coch}}^{(k)} + I_{\text{res}}^{(k)}} \right) ,$$

where the interference also includes the term $I_{\text{coch}}^{(k)}$, which takes into account the presence of two other beams sharing the same frequency inside the hotspot (see Fig. 14).

The achievable rate by configuration ℓ is simply the sum of the 7 rates, computed as in (14), and the throughput is computed as

$$\text{Throughput}^{(\ell)} = I_R^{(\ell)} 2B/3 \text{ [bit/s]}\,.$$

Since in this scenario it does not make sense to define a C/I_1 value, we sort the users and define the coverage area inside the beam according to their received power, C. After averaging on many configurations of users' positions, we can compute the throughput for different values of C. The results are reported in Fig. 15, where we notice that, also in this case, the best performance is achieved by serving almost the whole beam with the central signal. The maximum value of the throughput, for this scenario, is

$$\text{Throughput}^{(\text{3-colors SUD})} = 9.67 \text{ Gbit/s}\,.$$

E. MUD/SUD with 6 users

This scenario adopts the same assumptions on the received power and interference as the MUD/SUD with 7 users. However, the detection strategy is different. This time, we assume that there are only 6 users served at the same time (instead of 7). Each of them is always served by one of the adjacent beams. The resources of the central beam are allocated to each of them in a time division fashion. Hence, one of the users sees the channel as a classical MAC, where two signals are intended for the same user. The rates of these two signals are jointly selected to maximize the sum-rate, still choosing the combination of rates that minimizes the rate from the central

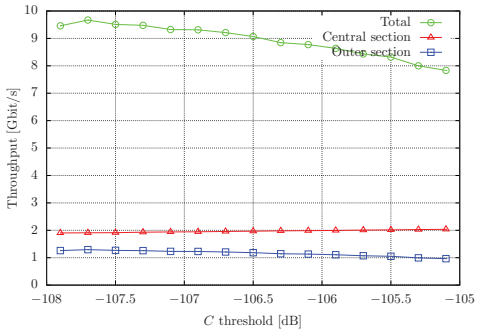

Figure 15. Throughput as a function of the C threshold for the inner and outer sections for the 3-color SUD.

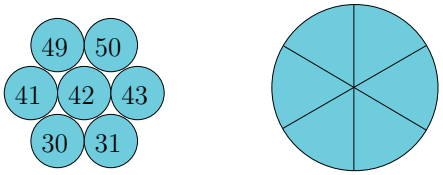

(a) (b)

Figure 16. Frequency reuse scheme (a) and beam coverage (b), for the MUD/SUD with 6 users.

beam. The other 5 users, instead, will perform exactly the same operations as in the previous MUD/SUD scenario: they will select their rate with a constraint on the rate of the first signal, which is fixed. The beam coverage is reported in Fig. 16.

As already done previously, let us denote by x_1 the signal transmitted on the central beam with rate R_1, and by x_k, $k = 2, \ldots, 7$, the signals transmitted by the 6 adjacent beams with rates R_k. Let us also define y_k the signal received by the user in the $k-$th section of the beam. The procedure to compute the achievable rates is schematically represented in Fig. 17, where $R_1^{(\mathrm{MUD})}$ is the minimum value of the rate of the central signal which ensures the maximum rate on the MAC for the first two signals (the channel with the closed red region). The other 5 users, instead, can select their rates R_k, $k = 3, \ldots, 7$, in the points of their open regions of abscissa $R_1^{(\mathrm{MUD})}$. The total sum-rate for a generic configuration ℓ of 6 users, in this case, is computed as

$$I_R^{(\ell)} = R_1^{(\mathrm{MUD})} + \sum_{k=2}^{7} R_k \, .$$

The technique described so far foresees the use of optimal

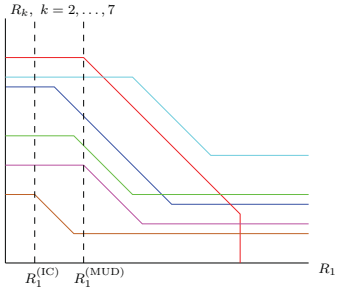

Figure 17. Examples of achievable rate regions for the 6 users solution.

multiuser detection, which, however, requires that the two streams are perfectly aligned in time (which might not always be true). A suboptimal solution relaxing this constraint is based on interference cancellation (IC) [38] and detection performed by means of a SUD: the signal coming from the central beam is detected first, and then canceled by all users. In this way, all signals are detected by means of single-user operations and can, in principle, work without the need of alignment of the symbols.

To perform interference cancellation, the rates of the 6 signals from the adjacent beams have to be selected on the horizontal borders of their regions, and have expression

$$R_k = I(x_k; y_k | x_1) \quad k = 2, \ldots, 7 \, .$$

To ensure that the rates R_k are achievable by all users, the rate R_1 must be selected as

$$R_1^{(\mathrm{IC})} = \min_{k=2,\ldots,7} I(x_1; y_k) \, ,$$

as graphically represented in Fig. 17. The total sum-rate for the generic configuration of users ℓ is

$$I_R^{(\ell)} = R_1^{(\mathrm{IC})} + \sum_{k=2}^{7} R_k \, .$$

In both cases, the throughput for the configuration ℓ has expression as in (7) and, after averaging over many configurations of 6 users, we find that the overall throughput for this scenario is

$$\mathrm{Throughput}^{(\mathrm{MUD/SUD\ 6\ users})} = 6.88 \ \mathrm{Gbit/s}$$

for the solution adopting the MUD, and

$$\mathrm{Throughput}^{(\mathrm{IC\text{-}SUD\ 6\ users})} = 6.58 \ \mathrm{Gbit/s}$$

for the solution adopting SUD and IC.

F. Discussion

Fig. 18 reports in a single plot the results obtained with the different strategies in the hotspot scenario. From the comparison, we notice that all proposed solutions exhibit a large gain with respect to the reference scenario. By comparing the alternative strategies, we see that, with the adopted power profiles and interference patterns, the 3-color SUD is the clear winner, gaining about 40% over the closest alternative, with a lower receiver complexity. If we compare the MUD/SUD options, we see that the solution with 6 users gains about 15% with respect to that with 7 users, and that using IC and SUD results in a loss of only 4% from the optimal MUD. We point out that these are bounds based on the assumptions of Gaussian inputs and linear channel. It is important to notice that the conclusions might change in presence of a more realistic model, including transponder nonlinearities and discrete symbols, although we believe that the winner strategy would remain the same. Further analyses in this direction are object of a future study. We also underline that the objective of this analysis has been to achieve the maximum throughput in the central beam. However, we can notice that the optimal solutions can result in a significantly unbalanced distribution

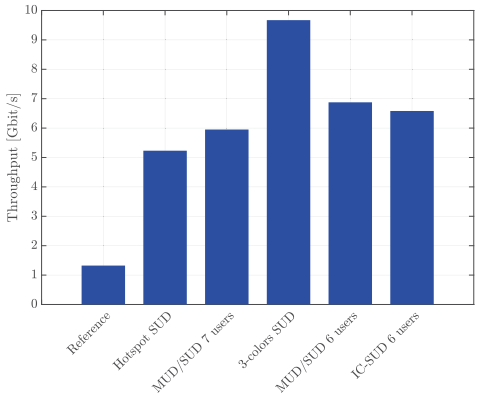

Figure 18. Throughput comparison of the described hotspot scenarios.

of the rates among the users in the beam. Let us consider, for example, the 3-color SUD, whose results are reported in Fig. 15. The maximum throughput is achieved by serving almost the whole beam with the central signal, and the average throughput received in the 7 sections has a similar value. However, more users have to share the achievable throughput in the central section with respect to the outer sections, hence the average throughput per user will be lower in the central section of the beam. An analysis aimed at ensuring a certain level of fairness among the throughput of each user would need a different optimization approach, however this was not the target of the performed study.

V. Conclusions

We have considered advanced schemes involving the application of multiuser detection to the forward link of a multibeam satellite system. First of all, we have proposed an information theoretical framework based on the combined use of single- and multiuser detection for two co-frequency users.

We have studied the maximization of the average throughput per beam in a typical multibeam scenario. We have compared 3 frequency reuse schemes, showing that the proposed framework, together with a scheme with 1 of 2 colors, can achieve significant performance gains with respect to a conventional solution, based on single-user detection in a 4-color scheme. The analysis has been carried out with a realistic channel model and discrete constellations, so the results can be considered as reliable bounds to the performance of practical coding schemes. Clearly, the proposed solution requires a complexity increase of the user terminals.

Then, we have used the same framework to analyze a hotspot scenario, where a beam with a high requirement is surrounded by beams with no requirement. Resources from the adjacent beams are pulled to the central beam, to increase the system flexibility. In this case, we have demonstrated that a 3-color scheme, together with single-user detection, is the best solution. This analysis has been performed under the assumption of Gaussian signals and linear channel. We have verified that, in these conditions, the strategies involving multiuser detection cannot provide advantages.

Appendix A
Proof of Theorem 1

We now prove Theorem 1.

Proof: Mathematically, we want to prove that the sum-rate $R_1 + R_2$ achievable by the MUD/SUD strategy is always greater than or equal to $R_{\mathrm{MAC,best}}$, defined as in (3). The proof can be simply done graphically, by considering the possible positions of the intersection of the achievable rate regions of both users. Fig. 19 shows all of the possible configurations of the capacity region of the two users. Let us analyze them one by one, observing that the same analysis is valid for the symmetric cases.

(a) The maximum sum-rate is achieved by using two SUDs, so $R_1 + R_2 = I(x_1; y_1) + I(x_2; y_2)$. Let us suppose that $R_{\mathrm{MAC,best}} = R_{\mathrm{MAC},1}$ (the case when $R_{\mathrm{MAC,best}} = R_{\mathrm{MAC},2}$ can be analyzed in the same way).

$$\begin{aligned} I(x_1; y_1) + I(x_2; y_2) &\geq R_{\mathrm{MAC},1} \\ &= I(x_1, x_2; y_1) \\ &= I(x_1; y_1) + I(x_2; y_1|x_1)\,. \end{aligned}$$

This is equivalent to $R_2 \geq I(x_2; y_1|x_1)$, which is clearly satisfied when the joint rate region has this shape.

(b) The maximum sum-rate is $R_1 + R_2 = I(x_1, x_2; y_1)$, which is also equal to $R_{\mathrm{MAC,best}}$, so the theorem is satisfied with equality.

(c) In this case, $I(x_2; y_2) < I(x_2; y_1)$, which is an unrealistic condition. This situation does not satisfy the stated realistic assumption.

(d) Also this case does not satisfy the assumption because $I(x_1; y_1) < I(x_1; y_2)$.

(e) The same happens in this case, $I(x_1; y_1) < I(x_1; y_2)$.

(f) Here,

$$\begin{aligned} R_1 + R_2 &= I(x_1, x_2; y_1) \\ &= I(x_1, x_2; y_2) \\ &= R_{\mathrm{MAC,best}}\,, \end{aligned}$$

and the condition is satisfied with equality.

By analyzing every possible configuration, we have proved the theorem in all cases in which $I(x_i; y_i) \geq I(x_i; y_{3-i})$, $i = 1, 2$. ■

References

[1] ETSI EN 302 307-1 Digital Video Broadcasting (DVB), Second generation framing structure, channel coding and modulation systems for Broadcasting, Interactive Services, News Gathering and other broadband satellite applications, Part I: DVB-S2.

[2] ETSI EN 302 307-2 Digital Video Broadcasting (DVB), Second generation framing structure, channel coding and modulation systems for Broadcasting, Interactive Services, News Gathering and other broadband satellite applications, Part II: S2-Extensions (DVB-S2X).

[3] A. Barbieri, D. Fertonani, and G. Colavolpe, "Time-frequency packing for linear modulations: spectral efficiency and practical detection schemes," *IEEE Trans. Commun.*, vol. 57, pp. 2951–2959, Oct. 2009.

[4] A. Piemontese, A. Modenini, G. Colavolpe, and N. Alagha, "Improving the spectral efficiency of nonlinear satellite systems through time-frequency packing and advanced processing," *IEEE Trans. Commun.*, vol. 61, pp. 3404–3412, Aug. 2013.

[5] A. Ugolini, Y. Zanettini, A. Piemontese, G. Colavolpe, and A. Vanelli-Coralli, "Efficient satellite systems based on interference management and exploitation," in *Proc. Asilomar Conf. Signals, Systems, Comp.*, (Pacific Grove, CA, USA), pp. 492–496, Nov. 2016.

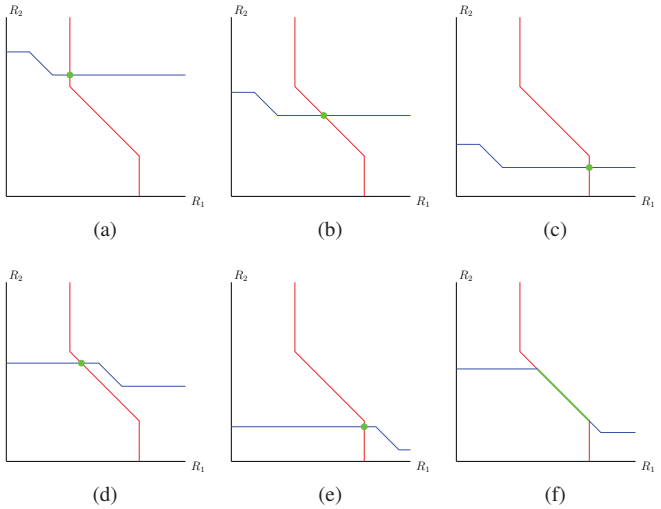

Figure 19. Graphical proof of Theorem 1.

[6] P.-D. Arapoglou, A. Ginesi, S. Cioni, S. Erl, F. Clazzer, S. Andrenacci, and A. Vanelli-Coralli, "DVB-S2X-enabled precoding for high throughput satellite systems," *International Journal of Satellite Communications and Networking*, vol. 34, pp. 439–455, May/June 2016.

[7] M. L. Moher, "Multiuser decoding for multibeam systems," *IEEE Trans. Veh. Tech.*, vol. 49, pp. 1226–1234, July 2000.

[8] B. F. Beidas, H. El Gamal, and S. Kay, "Iterative interference cancellation for high spectral efficiency satellite communications," *IEEE Trans. Commun.*, vol. 50, pp. 31–36, Jan. 2002.

[9] N. Letzepis and A. J. Grant, "Capacity of the multiple spot beam satellite channel with Rician fading," *IEEE Trans. Inform. Theory*, vol. 54, pp. 5210–5222, Nov. 2008.

[10] G. Colavolpe, D. Fertonani, and A. Piemontese, "SISO detection over linear channels with linear complexity in the number of interferers," *IEEE J. Sel. Topics in Signal Proc.*, vol. 5, pp. 1475–1485, Dec. 2011.

[11] J. Arnau and C. Mosquera, "Multiuser detection performance in multibeam satellite links under imperfect CSI," in *Proc. Asilomar Conf. Signals, Systems, Comp.*, (Pacific Grove, CA), pp. 468–472, Nov. 2012.

[12] A. Piemontese, A. Graell i Amat, and G. Colavolpe, "Frequency packing and multiuser detection for CPMs: how to improve the spectral efficiency of DVB-RCS2 systems," *IEEE Wireless Commun. Letters*, vol. 2, pp. 74–77, Feb. 2013.

[13] D. Christopoulos, S. Chatzinotas, J. Krause, and B. Ottersten, "Multiuser detection in multibeam mobile satellite systems: A fair performance evaluation," in *Proc. Vehicular Tech. Conf.*, (Dresden, Germany), pp. 1–5, June 2013.

[14] G. Colavolpe, A. Modenini, A. Piemontese, and A. Ugolini, "Multiuser detection in multibeam satellite systems: Theoretical analysis and practical schemes," *IEEE Trans. Commun.*, vol. 65, pp. 945–955, Feb. 2017.

[15] G. Colavolpe, A. Modenini, A. Piemontese, and A. Ugolini, "On the application of multiuser detection in multibeam satellite systems," in *Proc. IEEE Intern. Conf. Commun.*, (London, UK), pp. 898–902, June 2015.

[16] M. Caus, A. I. Perez-Neira, M. Angelone, and A. Ginesi, "An innovative interference mitigation approach for high throughput satellite systems," in *Proc. IEEE Intern. Work. on Signal Processing Advances for Wireless Commun.*, (Stockholm, Sweden), pp. 515–519, June-July 2015.

[17] M. Angelone, A. Ginesi, M. Caus, A. I. Perez-Neira, and J. Ebert, "System performance of an advanced multi-user detection technique for high throughput satellite systems," in *Proc. 21st Ka and Broadband Commun. Conf.*, (Bologna, Italy), Oct. 2015.

[18] G. Cocco, M. Angelone, and A. I. Perez-Neira, "Co-channel interference cancellation at the user terminal in multibeam satellite systems," in *Proc. 7th Advanced Satell. Mobile Syst. Conf. and 13th Intern. Workshop on Signal Proc. for Space Commun. (ASMS&SPSC 2014)*, (Livorno, Italy), pp. 43–50, Sept. 2014.

[19] S. Andrenacci, M. Angelone, E. A. Candreva, G. Colavolpe, A. Ginesi, F. Lombardo, A. Modenini, C. Morel, A. Piemontese, and A. Vanelli-Coralli, "Physical layer performance of multi-user detection in broadband multi-beam systems based on DVB-S2," in *Proc. European Wireless (EW 2014)*, (Barcelona, Spain), May 2014.

[20] K. Plimon, J. Ebert, N. Stamenic, H. Schlemmer, M. Caus, W. Gappmair, M. Angelone, and A. Ginesi, "Multi-user detection performance demonstrator for realistic high throughput satellite systems," in *Proc. Int. Symposium on Communication Systems, Networks Digital Signal Processing (CSNDSP)*, (Budapest, Hungary), July 2018.

[21] C. Sacchi, T. F. Rahman, C. Stallo, and M. Ruggieri, "Evolutionary algorithms for near-optimum detection of multi-beam satellite signals," in *Proc. IEEE Aerospace Conference*, (Big Sky, MT, USA), Mar. 2018.

[22] N. A. K. Beigi and M. R. Soleymani, "Increasing bandwidth efficiency in multibeam satellite systems under interference limited condition using overlay coding," in *Proc. IEEE Vehicular Technology Conference (VTC Spring)*, (Sydney, Australia), June 2017.

[23] W. Nam, D. Bai, J. Lee, and I. Kang, "Advanced interference management for 5G cellular networks," *IEEE Commun. Mag.*, vol. 52, pp. 52–60, May 2014.

[24] M. Caus, M. A. Vazquez, and A. Perez-Neira, "NOMA and interference limited satellite scenarios," in *Proc. Asilomar Conf. Signals, Systems, Comp.*, (Pacific Grove, CA, USA), pp. 497–501, Nov. 2016.

[25] M. A. Vazquez, M. Caus, and A. Perez-Neira, "Performance analysis of joint precoding and MUD techniques in multibeam satellite systems," in *Proc. IEEE Global Telecommun. Conf.*, (Washington, DC, USA), Dec. 2016.

[26] N. Alagha and A. Modenini, "On capacity measures for multi-beam satellite systems analyses," in *Proc. 8th Advanced Satell. Mobile Syst. Conf. and 14th Intern. Workshop on Signal Proc. for Space Commun. (ASMS&SPSC 2016)*, (Palma de Mallorca, Spain), Sept. 2016.

[27] R. De Gaudenzi, N. Alagha, M. Angelone, and G. Gallinaro, "Exploiting code division multiplexing with decentralized multi user detection in the satellite multibeam forward link," *Intern. J. of Sat. Commun. and Network.*, Aug. 2017.

[28] V. Icolari, S. Cioni, P. D. Arapoglou, A. Ginesi, and A. Vanelli-Coralli, "Flexible precoding for mobile satellite system hot spots," in *Proc. IEEE Intern. Conf. Commun.*, (Paris, France), May 2017.

[29] A. Ugolini, G. Colavolpe, and A. Vanelli-Coralli, "A system level approach to the application of multiuser detection in multibeam satellite systems," in *Proc. Int. Symposium on Wireless Communication Systems*, (Bologna, Italy), Aug. 2017.

[30] G. Karam and H. Sari, "Analysis of predistortion, equalization, and ISI cancellation techniques in digital radio systems with nonlinear transmit amplifiers," *IEEE Trans. Commun.*, vol. 37, pp. 1245–1253, Dec 1989.

[31] S. Cioni, G. Colavolpe, V. Mignone, A. Modenini, A. Morello, M. Ricciulli, A. Ugolini, and Y. Zanettini, "Transmission parameters optimization and receiver architectures for DVB-S2X systems," *International Journal of Satellite Communications and Networking*, vol. 34, pp. 337–350, May/June 2016. Article first published online: June 2015.

[32] T. M. Cover and J. A. Thomas, *Elements of Information Theory*. New York: John Wiley & Sons, 2nd ed., 2006.

[33] D. M. Arnold, H.-A. Loeliger, P. O. Vontobel, A. Kavčić, and W. Zeng, "Simulation-based computation of information rates for channels with memory," *IEEE Trans. Inform. Theory*, vol. 52, pp. 3498–3508, Aug. 2006.

[34] N. Merhav, G. Kaplan, A. Lapidoth, and S. Shamai, "On information rates for mismatched decoders," *IEEE Trans. Inform. Theory*, vol. 40, pp. 1953–1967, Nov. 1994.

[35] H. Meyr, M. Oerder, and A. Polydoros, "On sampling rate, analog prefiltering, and sufficient statistics for digital receivers," *IEEE Trans. Commun.*, vol. 42, pp. 3208–3214, Dec. 1994.

[36] J. Munkres, "Algorithms for the assignment and transportation problems," *Journal of the Society for Industrial and Applied Mathematics*, vol. 5, no. 1, pp. 32–38, 1957.

[37] http://www.tlc.unipr.it/ugolini/hotspot_data.ods.

[38] P. D. Alexander, A. J. Grant, and M. C. Reed, "Iterative detection on code-division multiple-access with error control coding," *European Trans. Telecommun.*, vol. 9, pp. 419–426, Oct. 1998.

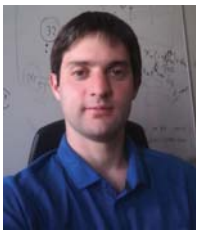

Alessandro Ugolini (M'16) was born in Parma, Italy, in 1987. He received the master's degree in Telecommunications Engineering (cum laude) from the University of Parma in 2012, and the Ph.D. degree in Information Technology from the same University in 2016. In 2012 he was awarded a National Inter-University Consortium for Telecommunications (CNIT) grant and a research grant funded by the Department of Information Engineering (DII), University of Parma, for the study of synchronization algorithms for spectrally efficient systems. In 2016 he has been a postdoctoral researcher at the DII. In 2017 he has been visiting researcher in the Communication and Antenna Systems division at Chalmers University of Technology, Gothenburg, Sweden, and at Interdisciplinary Centre for Security, Reliability and Trust, University of Luxembourg. Since 2017 he is a researcher at the Department of Engineering and Architecture (DIA) of the University of Parma. His main research interests include digital communications, applied information theory and synchronization.

Giulio Colavolpe (S'96–M'00–SM'11) was born in Cosenza, Italy, in 1969. He received the Dr. Ing. degree in Telecommunications Engineering (cum laude) from the University of Pisa, Italy, in 1994 and the Ph.D. degree in Information Technologies from the University of Parma, Italy, in 1998. Since 1997, he has been at the University of Parma, Italy, where he is now Professor of Telecommunications at the Dipartimento di Ingegneria e Architettura (DIA). In 2000, he was Visiting Scientist at the Institut Eurécom, Valbonne, France. His research interests include the design of digital communication systems, adaptive signal processing (with particular emphasis on iterative detection techniques for channels with memory), channel coding and information theory. His research activity has led to more than 200 papers in refereed journals and in leading international conferences, and 18 industrial patents. He received the best paper award at the 13th International Conference on Software, Telecommunications and Computer Networks (SoftCOM'05), Split, Croatia, September 2005, the best paper award for Optical Networks and Systems at the IEEE International Conference on Communications (ICC 2008), Beijing, China, May 2008, and the best paper award at the 5th Advanced Satellite Mobile Systems Conference and 11th International Workshop on Signal Processing for Space Communications (ASMS&SPSC 2010), Cagliari, Italy. He served as an Editor for IEEE Transactions on Wireless Communications, IEEE Transactions on Communications, and IEEE Wireless Communications Letters and as an Executive Editor for Transactions on Emerging Telecommunications Technologies (ETT).

Martina Angelone Martina Angelone received her M.S. degree (summa cum laude) in telecommunication engineering from the University of Pisa, Italy, in 2008. In 2009 she joined M.B.I. s.r.l., an ICT company in Pisa, as a communication system engineer. In 2010, she was a Young Graduate Trainee with the European Space Agency (ESA) at the European Space Research and Technology Centre (ESTEC), Noordwijk, The Netherlands, where she focused on the end-to-end performance analysis of satellite communication systems. She then joined in 2011 the Communication systems and techniques section of the RF Payload system division. She has been responsible of several R&D ARTES projects related to broadband satellite systems, advanced interference mitigation techniques as well as for the development of hardware for high rate TT&C applications and she has supported many activities from a system point of view. She has contributed to several standardization technical groups including DVB-S2X and DVB-RCS2. Since August 2018 she is the System Engineer of the IRIS programme of the Telecommunications and Integrated Applications Directorate (TIA), targeting the development satellite-based air–ground communication system for Air Traffic Management (ATM).

Alessandro Vanelli-Coralli (S'93–M'97–SM'07) received the Dr.Ing. degree in electronics engineering and the Ph.D. degree in electronics and computer science from the University of Bologna, Italy, in 1991 and 1996, respectively. In 1996, he joined the University of Bologna, where he is currently an Associate Professor with the Department of Electrical, Electronic, and Information Engineering (Guglielmo Marconi). He chaired the Ph.D. Board, Electronics, Telecommunications and Information Technologies from 2013 to 2018. From 2003 to 2005, he was a Visiting Scientist with Qualcomm Inc., San Diego, CA, USA. He participates in national and international research projects on wireless and satellite communication systems. He has been a Project Coordinator and scientific responsible for several European Space Agency and European Commission funded projects. His research interests include wireless communications, digital transmission techniques, and digital signal processing. He was a co-recipient of several best paper awards. He has served as the general chairman and the technical chairman for several scientific conferences. He has been an appointed member of the Editorial Board of the International Journal of Satellite Communications and Networking (Wiley InterScience) and has been a guest co-editor for several special issues of the international scientific journals.

Alberto Ginesi was born in Parma, Italy, in November 1967. He received the Dr. Ing. (cum laude) and PhD degrees in electronic engineering from the University of Pisa, Italy, in 1993 and 1998, respectively. In 1996–1997, he spent 1 year at Carleton University, Ottawa, Canada, performing research in digital transmissions for wireless applications. In 1997, he joined Nortel Networks and in 2000 Catena Networks, both in Ottawa, Canada, where he worked on Digital Subscriber Loop (DSL) technologies and contributed to the definition of the second–generation ADSL standards in the context of the ITU–R standardization body. Since 2002, he is with the Research and Technology Centre (ESTEC) of the European Space Agency (ESA) at Noordwijk, The Netherlands, where he is currently the Head of the Telecommunication–TT&C Systems and Techniques Section of the Technical and Quality Management Directorate, being responsible for the R&D of satellite telecommunication and TT&C systems. His main research interests are in the area of advanced digital communication systems and techniques from theory to hardware implementation. Dr Ginesi is coauthor of more than 50 scientific publications and more than 20 international patents on subjects covering both DSL and satellite communication systems.